

AVERAGE AND SMALL SIGNAL MODELING OF ZERO-VOLTAGE TRANSITION THREE-PHASE PWM BOOST RECTIFIER

Ravindra Ambatipudi, Dushan Boroyevich, Silva Hiti, and Fred. C. Lee

Virginia Power Electronics Center
The Bradley Department of Electrical Engineering
Virginia Polytechnic Institute and State University
Blacksburg, Virginia 24061

Abstract - Average and small signal modeling of zero-voltage transition three-phase boost rectifier is performed. The effect of ZVT is introduced in the existing model for the three-phase boost rectifier using the time-averaging equivalent circuit approach. The small signal model is derived from the average model. The small signal characteristics are compared to the corresponding characteristics without ZVT.

1. INTRODUCTION

Switching losses have become a major concern in all applications requiring high switching frequency. Hence soft switching has become a necessity in all high power applications, especially in three-phase power conversion. Several soft-switched three-phase PWM boost rectifiers have been presented in [1]. A very attractive topology is based on zero-voltage transition (ZVT) technique [2], and is shown in Fig. 1.

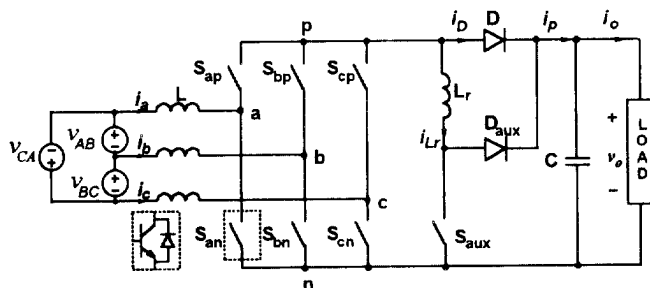


Fig. 1 ZVT Three phase PWM boost rectifier

It was shown in [3] and [4] that the small signal characteristics of a dc/dc converter change significantly with the introduction of zero-voltage switching. Although the three phase boost rectifier has been modeled in [5] and [6], no effort has been made to analyze the effect of zero-voltage switching on small signal characteristics. The objective of this paper is to

analyze the effect of ZVT on the small signal characteristics of the converter shown in Fig. 1. The average model developed in [6] is modified to include ZVT similarly as was done for the modeling of the ZVT dc/dc boost converter using the time-averaging equivalent circuit approach [7]. The small signal model is derived from the average model and the transfer functions are compared to the corresponding transfer functions of the conventional three-phase boost rectifier to show the effect of ZVT.

2. PRINCIPLE OF OPERATION

The ZVT three-phase PWM boost rectifier is different from the conventional one due to the presence of the auxiliary network on the dc side. The dc-rail diode, D, isolates the output capacitor and the load from the bridge when the ZVT circuit (consisting of L_r , S_{aux} and D_{aux}) is activated. The auxiliary network operates only during the short turn-on transient to provide the soft switching.

The operation principle is illustrated for the circuit in Fig. 1 operating with six-step PWM (space vector modulation) and unity power factor [1]. Consider the 60° interval within the input line period when $i_a > 0$, $i_b \leq 0$, $i_c \leq 0$. During this interval switches S_{ap} and S_{an} are disabled, and the current i_a flows through the anti-parallel diode of the switch S_{ap} . In order to activate the ZVT circuit only once during the switching period, turn-on instants of the switches S_{bp} and S_{cp} are synchronized. Fig. 2 shows the relevant voltage and current waveforms.

Prior to time T_0 , the anti-parallel diodes of the switches S_{ap} , S_{bn} , S_{cn} , and the diode D are conducting. S_{aux} is turned on at time T_0 . Current through the diode D starts decreasing and the current through L_r linearly

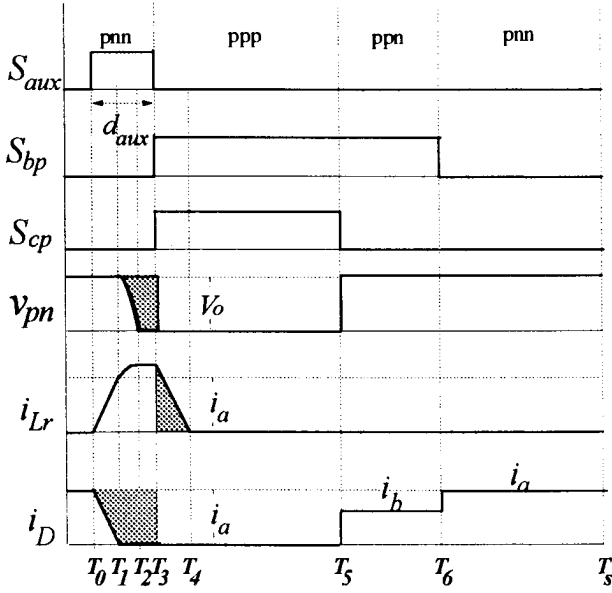


Fig. 2 Circuit waveforms within one switching cycle when $i_a > 0$, $i_b \leq 0$, $i_c \leq 0$

ramps up until it reaches the input phase current i_a . Diode D is turned off softly at time T_1 . This time interval is given by

$$T_1 - T_0 = \frac{L_r I_m}{v_o}, \quad (1)$$

where I_m is the largest input current in the present 60° interval and v_o is the output voltage.

If the diode D is a fast recovery diode, then its reverse recovery current will be negligible because of the controlled dv/dt and di/dt at turn-off. After time T_1 , current through L_r continues to increase due to resonance between L_r and the equivalent capacitance across the bridge, C_r . During this time the bridge output voltage, v_{pn} , decreases in a resonant fashion until it reaches zero at time T_2 , when the anti-parallel diodes of S_{an} , S_{bp} and S_{cp} start conducting. At that moment switches S_{bp} and S_{cp} can be turned on under zero voltage conditions. This resonant period is given by

$$T_2 - T_1 = \frac{\pi}{2} \sqrt{L_r C_r}. \quad (2)$$

S_{aux} is turned off at T_3 and its voltage is clamped to the output voltage due to the conduction of D_{aux} . The duty cycle of the auxiliary switch, d_{aux} , which determines the delay between the auxiliary switch and the main switch turn-on, has to satisfy the following condition in order to achieve zero-voltage switching:

$$d_{aux} T_s \geq (T_1 - T_0) + (T_2 - T_1), \quad (3)$$

where $T_1 - T_0$ and $T_2 - T_1$ are given by (1) and (2) respectively, and T_s is the total switching period.

After time T_3 , the energy stored in the inductor is transferred to the output capacitor through D_{aux} . D_{aux} stops conducting at time T_4 when the energy stored in L_r is completely transferred to the capacitor. This time interval is given by:

$$T_4 - T_3 = \left(\frac{L_r I_m}{v_o} + \sqrt{L_r C_r} \right). \quad (4)$$

The operation of the circuit after time T_4 is same as its PWM counterpart. The circuit operation and the waveforms are cyclically symmetrical during other 60° intervals.

3. CONVERTER MODELING

The average model of the three phase boost rectifier is developed in the same way as for its PWM counterpart [6]. The effect of ZVT is introduced by time-averaging equivalent circuit approach, [3] and [7], which is an extension of state space averaging approach.

If in the above example the ZVT circuit were not activated, the average line voltages at the bridge input would be, [6],

$$v_{ab} = d_{ab} \cdot v_o, \quad v_{bc} = d_{bc} \cdot v_o, \quad v_{ca} = d_{ca} \cdot v_o. \quad (5)$$

In (5) $d_{ab} = d_a - d_b$, $d_{bc} = d_b - d_c$ and $d_{ca} = d_c - d_a$, where d_i ($i=a,b,c$) are duty cycles of the switches S_{ip} . Due to the action of ZVT circuit, $d_{ab} \cdot v_o$ decreases and $d_{ca} \cdot v_o$ increases by the average value of the shaded area in the waveform of v_{pn} in Fig. 2. This shaded area can be easily calculated from Fig. 2 and the effective change in duty cycles is given by

$$\Delta d = d_{aux} - \frac{T_1 - T_0}{T_s} - \frac{2}{\pi} \frac{T_2 - T_1}{T_s}. \quad (6)$$

In (6), $T_1 - T_0$ and $T_2 - T_1$ are given by (1) and (2) respectively. The change in effective duty cycle, Δd , is the same throughout the 60° interval and changes cyclically within the line period. As a result, the average model of the three-phase PWM boost rectifier can be modified so that

$$\begin{aligned} v_{ab} &= (d_{ab} - f_{ab} \cdot \Delta d) v_o, \quad v_{bc} = (d_{bc} - f_{bc} \cdot \Delta d) v_o, \\ v_{ca} &= (d_{ca} - f_{ca} \cdot \Delta d) v_o. \end{aligned} \quad (7)$$

where f_{ab} , f_{bc} and f_{ca} model the cyclical change in duty cycles and are shown in Fig. 3.

Similarly, the average value of the current supplying the output capacitor and the load without ZVT would be, [6],

$$i_p = d_{ab} \cdot i_{ab} + d_{bc} \cdot i_{bc} + d_{ca} \cdot i_{ca},$$

where

$$i_{ab} = (i_a - i_b)/3, \quad i_{bc} = (i_b - i_c)/3, \quad i_{ca} = (i_c - i_a)/3.$$

With ZVT this current not only decreases by the amount i_{DS} , which is the shaded part of the waveform of i_D in Fig. 2, but also has an additional component through the diode D_{aux} which is equal to the shaded part of the waveform of i_{Lr} in Fig. 2, i.e.

$$i_p = (d_{ab} \cdot i_{ab} + d_{bc} \cdot i_{bc} + d_{ca} \cdot i_{ca}) - i_x, \quad (8)$$

where

$$i_x = i_{DS} - i_{Lrs}. \quad (9)$$

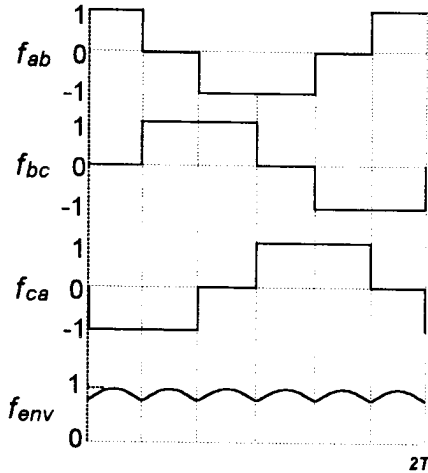


Fig. 3 f_{ab} , f_{bc} , f_{ca} , and f_{env} waveforms

The components i_{DS} and i_{Lrs} can be easily derived from Fig. 2 and are given by

$$i_{DS} = \left(d_{aux} - \frac{T_1 - T_0}{2T_s} \right) I_m, \quad (10)$$

$$i_{Lrs} = \frac{T_4 - T_3}{2T_s} \left(I_m + \frac{v_o}{\sqrt{L_r/C_r}} \right). \quad (11)$$

In (10) and (11), $T_1 - T_0$ and $T_4 - T_3$ are given by (1) and (4) respectively. I_m is the instantaneous peak value of the current charging the output capacitor. This value varies during consecutive 60° intervals as shown

by the function f_{env} in Fig. 3. Then I_m can be expressed in terms of the amplitude of input currents, I_p , and f_{env} as follows:

$$I_m = f_{env} \cdot I_p \quad (12)$$

The remaining part of the circuit in Fig. 1 is linear and can be described by, [6],

$$\begin{aligned} v_{AB} &= 3L \frac{di_{ab}}{dt} + v_{ab}, \\ v_{BC} &= 3L \frac{di_{bc}}{dt} + v_{bc}, \\ v_{CA} &= 3L \frac{di_{ca}}{dt} + v_{ca}, \end{aligned} \quad (13)$$

and

$$i_p = C \frac{dv_o}{dt} + i_o. \quad (14)$$

Equations (6) to (14), together with (1), (2), and (3) represent the average model of the ZVT three-phase PWM boost rectifier shown in Fig. 1, in stationary coordinates.

4. AVERAGE MODEL IN ROTATING COORDINATES

The average model in stationary coordinates cannot be linearized to give a small signal model as the variables are sinusoidal in steady state. Hence the model is transformed to rotating reference frame using d-q transformation, [5], [6]. However, d-q transformation of the functions in Fig. 3 would also result in time varying variables in steady state. The approximate models can be derived if the functions f_{ab} , f_{bc} and f_{ca} are substituted by their first harmonics before the coordinate transformation. The first harmonics of f_{ab} , f_{bc} and f_{ca} are given by

$$\begin{aligned} f_{ab} &= \frac{2\sqrt{3}}{\pi} \cos(\omega t), \\ f_{bc} &= \frac{2\sqrt{3}}{\pi} \cos\left(\omega t - \frac{2\pi}{3}\right), \\ f_{ca} &= \frac{2\sqrt{3}}{\pi} \cos\left(\omega t + \frac{2\pi}{3}\right). \end{aligned} \quad (15)$$

The function f_{env} is represented with its average value, $3/\pi$. The resulting model in rotating reference frame is shown in Fig. 4. The angular frequency of the

rotating reference frame is equal to the line frequency $2\pi f_i$, and d-axis is aligned with the voltage v_{ab} . Variables f_{ab} , f_{bc} and f_{ca} are also transformed into d-q frame and the corresponding d and q components are given by

$$f_d = \frac{2\sqrt{3}}{\pi}, f_q = 0. \quad (16)$$

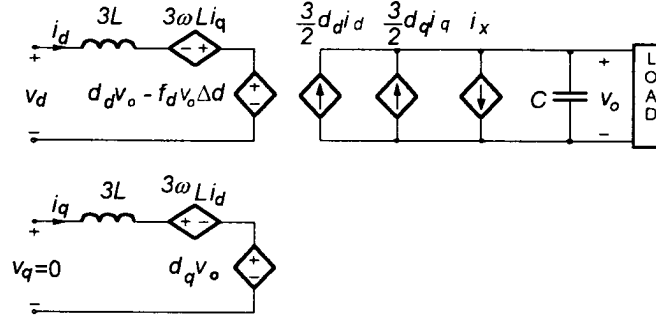


Fig. 4 Average Model in rotating coordinates

5. SMALL SIGNAL MODELING

The average model shown in Fig. 4 can be linearized to give a linear time-invariant small signal model. The linearized equations are shown below:

$$\begin{aligned} \frac{d\hat{i}_d}{dt} &= \omega \hat{i}_q - \frac{V_o}{3L} \hat{d}_d + \left(\frac{D_d}{3L} + \frac{f_d \cdot \Delta d}{3L} \right) \hat{v}_o \\ &\quad + \frac{f_d \cdot V_o}{3L} \Delta \hat{d}, \end{aligned} \quad (17)$$

$$\frac{d\hat{i}_q}{dt} = -\omega \hat{i}_d - \frac{V_o}{3L} \hat{d}_q - \frac{D_q}{3L} \hat{v}_o, \quad (18)$$

$$\frac{d\hat{v}_o}{dt} = \frac{3D_d}{2C} \hat{i}_d + \frac{3I_d}{2C} \hat{d}_d + \frac{3D_q}{2C} \hat{i}_q - \frac{1}{C} \hat{i}_x, \quad (19)$$

where

$$\Delta \hat{d} = d_{aux} - \frac{3L_r}{\pi T_s} \left(\frac{1}{V_o} \hat{i}_d - \frac{I_d}{V_o^2} \hat{v}_o \right), \quad (20)$$

and

$$\begin{aligned} \hat{i}_x &= \left[\frac{3d_{aux}}{\pi} - \frac{3\sqrt{L_r C_r}}{\pi T_s} - \frac{18L_r I_d}{\pi^2 V_o T_s} \right] \hat{i}_d \\ &\quad + \left(\frac{9L_r I_d^2}{\pi^2 V_o^2 T_s} - \frac{C_r}{T_s} \right) \hat{v}_o. \end{aligned} \quad (21)$$

To study the effect of ZVT, this small signal model was simulated for a 5 kW converter (parameters are in Appendix A) and the results were compared with

the corresponding results for PWM converter. The above equations are derived under the assumption of unity input displacement factor, when the steady state value of the direct component of the input current, I_d is equal to I_p , the amplitude of the input phase currents, and the quadrature component, I_q is zero. In (17) -(21) uppercase letters denote steady state values, while the symbol, ^ denotes small-signal perturbation.

Fig. 5 shows all the control to output transfer functions required for control design, with and without ZVT. There is a slight decrease in the dc gain, and significant increase in damping introduced by ZVT. This result is in agreement with previous results for dc/dc converters, [3], [4]. The ZVT introduces feedback in \hat{i}_d and \hat{v}_o through $\Delta \hat{d}$ and \hat{i}_x . The term proportional to \hat{v}_o in (20) results in the change of dc gain in (17) while the term proportional to \hat{i}_d in (20) introduces damping in (17). Similarly, the term proportional to \hat{i}_d in (21) effects the dc gain in (19) and the term proportional to \hat{v}_o results in damping of (19).

6. CONCLUSIONS

In order to enable analysis and control design of the ZVT three-phase boost rectifier, average and small signal modeling was performed. It is shown that small signal characteristics of the three-phase boost rectifier vary appreciably due to ZVT.

The ZVT action has two effects:

- I. It changes the dc value of the duty cycle
- II. It introduces feedback from the output voltage and direct component of the input current

The most pronounced consequences are that the first effect limits the maximum duty cycle to some value less than unity, while the second effect significantly increases transfer function damping..

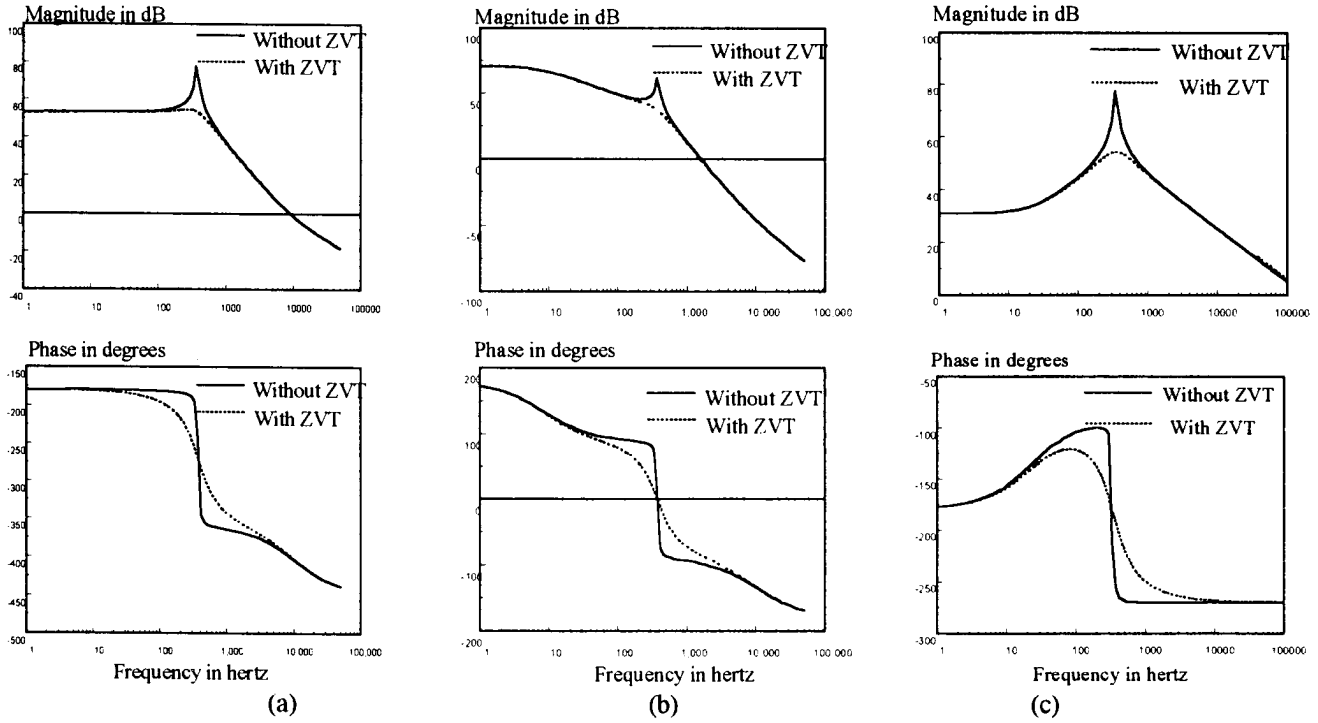


Fig. 5 Small signal transfer functions (a) \hat{v}_o/\hat{d}_d , (b) \hat{v}_o/\hat{d}_q , (c) \hat{i}_d/\hat{d}_d

The ZVT effects do not change sinusoidally nor they are constant in steady state. In order to obtain time-invariant d-q model, only the first order effects of ZVT were taken into account. The resulting approximation should not cause large errors, especially in the linearized model. Additional assumptions used in the model derivations are that all components in Fig. 1 are ideal, and that the circuit operates with unity displacement factor.

APPENDIX A

Power stage parameters:

input line rms voltage 180 V, $V_o = 350$ V, $L = 100$ μ H,
 $C = 500$ μ F, $L_r = 5$ μ H, $C_r = 25$ nF, $f_s = 100$ kHz, $f_l = 60$ Hz,
 $R_{load} = 25$ Ω , $d_{aux} = 0.1$.

REFERENCES

- [1] Y. Jiang, H. Mao, F.C. Lee, and D. Boroyevich, "Simple high performance three phase boost rectifiers," *Proc. IEEE PESC 94*, pp. 1158-1163, 1994.
- [2] G.C. Hua, C.S. Leu, and F.C. Lee, "Novel zero-voltage transition PWM converter," *Proc. IEEE PESC 92*, pp. 55-61, 1992.
- [3] G.C. Hua, "Soft switched PWM converters," *Ph.D dissertation*, Blacksburg: Virginia Polytechnic Institute and State University, 1994.
- [4] V. Vlatkovich, J.A. Sabate, R.B. Ridley, F.C. Lee, and B.H. Cho, "Small-signal analysis of zero-voltage switched full-bridge PWM converter," *HFPC Conf. Rec.*, pp. 262-272, 1990.
- [5] C.T. Rim, D.Y. Hu, and G.H. Cho, "Transformers as equivalent circuits for switches: General proofs and d-q transformation-based analysis," *IEEE Trans. on Industry Applications*, Vol. 26, no. 4, pp. 777-785, 1990.
- [6] S. Hiti and D. Boroyevich, "Control of front end three phase boost rectifier," *Proc. IEEE APEC 94*, pp. 927-933, 1994.
- [7] J. Xu, "Modeling of switching dc-dc converters by time-averaging equivalent circuit approach," *Int. J. Electronics*, Vol. 74, no. 3, 1993.